



ELSEVIER

8 October 1998

PHYSICS LETTERS B

Physics Letters B 437 (1998) 257–263

Measurement of quasi-elastic $^{12}\text{C}(p,2p)$ scattering at high momentum transfer

Y. Mardor ^a, J. Aclander ^a, J. Alster ^a, D. Barton ^b, G. Bunce ^b, A. Carroll ^b,
N. Christensen ^{c,1}, H. Courant ^c, S. Durrant ^{a,b}, S. Gushue ^b, S. Heppelmann ^d,
E. Kosonovsky ^a, I. Mardor ^a, M. Marshak ^c, Y. Makdisi ^b, E.D. Minor ^{d,2},
I. Navon ^a, H. Nicholson ^e, E. Piassetzky ^a, T. Roser ^b, J. Russell ^f, C.S. Sutton ^e,
M. Tanaka ^{b,3}, C. White ^c, J-Y Wu ^{d,4}

^a School of Physics and Astronomy, Sackler Faculty of Exact Sciences, Tel Aviv University, Israel

^b Brookhaven National Laboratory, USA

^c Physics Department, University of Minnesota, USA

^d Physics Department, Pennsylvania State University, USA

^e Mount Holyoke College, USA

^f Physics Department, University of Massachusetts Dartmouth, USA

Received 24 March 1998; revised 18 June 1998

Editor: J.P. Schiffer

Abstract

We measured the high-momentum transfer [$Q^2 = 4.8$ and 6.2 (GeV/c) 2] quasi-elastic $^{12}\text{C}(p,2p)$ reaction at $\theta_{\text{cm}} \approx 90^\circ$ for 6 and 7.5 GeV/c incident protons. The momentum components of both outgoing protons and the missing energy and momentum of the proton in the nucleus were measured. We verified the validity of the quasi-elastic picture for ground state momenta up to about 0.5 GeV/c. Transverse and longitudinal momentum distributions of the target proton were measured. They have the same shape with a large momentum tail which is not consistent with independent particle models. We observed that the transverse distribution gets wider as the longitudinal component increases in the beam direction. © 1998 Elsevier Science B.V. All rights reserved.

PACS: 25.40.-h; 25.40.Ve; 24.10.-i; 24.50.+g

In quasi-elastic (QE) scattering, a projectile is elastically scattered from a single bound “target” nucleon in the nucleus while the rest of the nucleus acts as a spectator. The measured missing momentum in either (p,2p) or (e,e’p) quasi-elastic scattering is determined by two basic effects. The first is the ground state momentum distribution of the nucleon in the nucleus. The second is the interaction between the incident nucleon or one of the final state nucle-

¹ Current address: Department of Physics, University of Auckland, New Zealand.

² Current address: “Concurrent Technologies Corporation”, Johnstown, PA, USA.

³ Deceased.

⁴ Current address: “Fermi National Accelerator Laboratory”.

ons with the rest of the nucleus. In the plane wave impulse approximation, only the first contribution is considered. The relative importance of these two processes becomes the central issue for “Color Transparency”, the QCD prediction which has attracted much attention in recent years [1,2]. “Color Transparency” models predict that the nuclear initial-final state interactions will vanish at asymptotically large momentum transfer. The nominal experimental signature for Color Transparency from the (p,2p) involves reduction in nuclear absorption with energy. This normalized energy dependence will be discussed in a forthcoming publication. This paper reports on the identification of QE events at high Q^2 and on the momentum distributions observed in the reaction $^{12}\text{C}(p,2p)$ at momentum transfers of 4.8 and 6.2 (GeV/c)².

High energy measurements of nucleon momentum distributions can be rather different from the lower energy measurements. At high energy it is convenient to characterize the nucleon distribution in a nucleus in terms of the longitudinal “light cone momentum fraction” $\alpha = (E_F - p_{Fz})/m$, and a transverse momentum 2-vector \mathbf{p}_{Ft} [3,4]. Here E_F is the total target nucleon energy, p_{Fz} is the z component of the target proton momentum and m is the proton mass. It is the light cone nuclear representation of the nucleus which would be most useful for describing relativistic nuclear collisions from the perspective of colliding nucleons. This formulation is similar to the construction of parton distribution functions which are used to characterize partons in a nucleon. In general, the relationship between the rest frame energy-momentum distribution and the “light cone” distributions is not trivial and depends on the dynamics of the strongly interacting bound system. While we work with relativistic kinematics and variables, in this work we use the standard non-relativistic description of the nucleus.

A majority of the experiments dealing with momentum distributions in nuclei have used the (e,e’p) reaction. The (p,2p) reaction is different in interesting ways. The (p,p) cross sections are larger and the radiative corrections are negligible compared to electron scattering. On the other hand, the larger (p,p) cross section increases the role of final state interactions. As pointed out by Farrar et al. [5], the (p,2p) process provides a powerful amplification of the

large longitudinal momentum tails because of the strong energy dependence of the pp elastic scattering, a s^{-10} variation in the 90° cross section with the Mandelstam variable s [6]. The data reported here are the first verification that this enhanced signal in the extreme regions of large momentum can indeed be separated from background. These results will also be the subject of a forthcoming publication.

While comparison to the many lower energy measurements of nucleon momentum distributions is interesting, the (e,e’p) measurement which has the most similar energy scale was recently reported [7] covering the kinematic range [$Q^2 = 1-6.8$ (GeV/c)²]. The authors showed that their results are consistent with a conventional QE model of the reaction. Those measurements were made in the region of light cone momentum corresponding to small total nucleon momentum. The measurement reported here extends to more extreme regions of light cone momentum where off-shell and bound nucleon effects might actually destroy the QE picture.

In order to verify the QE picture, we study distributions at two incident momenta, 6.0 and 7.5 GeV/c. We will show that, to within the experimental errors of this measurement, the QE picture is applicable over the measured kinematical range and, consequently, that it should be possible to separate nuclear properties from the reaction mechanism. We will present and compare transverse and longitudinal momentum distributions of the target proton and compare both to the simplest independent particle models.

We measured the high-momentum transfer quasi-elastic C(p,2p) reaction at $\theta_{\text{cm}} \approx 90^\circ$ on carbon in a kinematically complete coincidence experiment. The three-momentum components of both high p_t final state protons were measured, which yielded the missing energy and momentum of the target proton in the nucleus. The experiment (E850) was performed at the AGS accelerator at Brookhaven National Laboratory with the EVA spectrometer [8–10]. The spectrometer consists of a super-conducting solenoidal magnet operated at 0.8 Tesla. The beam enters along the z axis and hits a series of targets located at various z positions. The scattered particles are tracked by four cylindrical chambers (C1–C4). The radii of the cylinders range from 10 to 180 cm. All

cylinders and targets can be moved along the solenoid axis in order to optimize the angular acceptance range for each beam momentum. Cylinders C2–C4 have 4 layers of 2 m long straw drift tubes, whose diameters range from 1 cm for C2 to 2 cm for C4. The high resistance central wires are read out at both ends, providing position information along the z direction. Thus, one can extract the z position of the particles in the cylinders as well as their azimuthal angles as they are bent in the axial magnetic field. This provides the transverse momentum of the particles and their scattering angle. The 1 m long C1 cylinder with a tube diameter of 0.5 cm was read out at one end only. The straw tubes were filled with a 1:1 mixture of argon-ethane gas at atmospheric pressure. The drift time measurement from the central wire had a spatial resolution of about 0.3 mm. Three solid targets, CH_2 , C and CD_2 (enriched to 95%) were placed on the z axis inside the C1 cylinder separated by about 20 cm. They were $5.1 \times 5.1 \text{ cm}^2$ squares and 6.6 cm long in the z direction except for the CD_2 target which was 4.9 cm long. Their positions were interchanged at several intervals in order to reduce systematic uncertainties and to maximize the acceptance range for each target. Only the C target was used to extract the QE events, while the other targets served for normalizations and references.

The spectrometer was located on the secondary line C1 of the AGS. The beam passed through a sequence of two differential Cerenkov counters which identified the incident particles. The beams ranged in intensity from 1 to $2 \cdot 10^7$ over a one second spill every 3 seconds. Two counter hodoscopes in the beam provided beam alignment and a timing reference. Three levels of triggering were used. The spectrometer included two fan-shaped arrays of scintillator hodoscopes which provided fast triggering of the first level by requiring a minimum transverse momentum. This trigger passed a typical event rate of 100 kHz. The second level trigger, which included some straw tube information, selected high transverse momentum and accepted a rate of 10 kHz. These hardware triggers selected events with transverse momenta $p_t > 0.8$ and $p_t > 0.9 \text{ GeV}/c$, for the 6 and 7.5 GeV/c measurements, respectively. The third level software trigger required two almost coplanar tracks, each satisfying the second level

trigger requirement and low multiplicity hits in the straw tubes. The accepted rate ranged from 10 to 40/sec. See ref [11] for a detailed description.

The coordinate system was chosen with the z coordinate in the beam direction and the y direction normal to the scattering plane (x, z). The latter is defined by the incident beam and one of the emerging protons. The selection among the two was random. This arbitrariness in the selection does not affect the extracted quantities of interest. The coordinates x and y are not fixed with respect to the spectrometer. The data were analyzed in terms of the momenta in the y direction (p_{Fy}) and the light cone α . This variable α is a natural choice for high energy reactions [3] and is also ideally adapted to our experimental analysis. We determined α with a precision of $\sigma \approx 3\%$. The p_{Fy} (perpendicular to the scattering plane) had a resolution of $\sigma = 40 \text{ MeV}/c$ and the resolution in p_{Fx} (in the scattering plane) was $\sigma = 170 \text{ MeV}/c$. Because of its better resolution, p_{Fy} was used to represent a transverse component. Both the α and p_{Fy} resolutions were determined by the elastic pp scattering events from the CH_2 target. The polar angles of both detected protons were limited by a software cut to a region of $\pm(3-5)^\circ$ around the center of the angular acceptance, for each target position. The angular range enforced by the software cut is smaller than the geometrical limits of the spectrometer but it ensures a uniform acceptance. We did not apply an explicit cut on the center of mass angle, however the cuts on the laboratory polar angles limit the θ_{cm} to the range of 83 to 90° .

The sample which contained the QE events had just two tracks in the detector with good track quality determined by the software cuts on the track reconstruction. The missing energy E_{miss} was obtained from the difference between the initial energy state of the beam plus proton mass and the two outgoing proton energies. In the QE picture E_{miss} is the single-particle binding energy of the target proton. Given the limited resolution for E_{miss} ($\sigma = 240 \text{ MeV}$), we applied a cut of $|E_{\text{miss}}| < 0.5 \text{ GeV}$. Since this cut is above m_π , some inelastic background, such as those coming from $pA \rightarrow pp\pi^0(A-1)$ events, could penetrate the cuts and had to be subtracted. The shape of this background was determined from a fit to the E_{miss} distribution of events

with extra tracks in the spectrometer. The p_{Fy} distribution was divided into bins. For each bin, separately, we fit the E_{miss} spectrum to the background and a Gaussian centered at $E_{\text{miss}} \approx 0$ which represents the QE events. The width of the Gaussian was determined from a fit to the peak at $E_{\text{miss}} \approx 0$ for $0 < p_{Fy} < 50$ MeV/c, where the peak is very prominent. An example is shown in Fig. 1. The reported α and p_{Fy} distributions are the results of these fits. The errors in Fig. 2 combine the statistical errors, which dominate, and the uncertainties due to background subtraction.

In Fig. 2 we present $|p_{Fy}|$ distributions. Figs. 2a and 2b show the p_{Fy} distributions for two regions of α , at 6 and 7.5 GeV/c. The curves were normalized at $p_{Fy} = 0$ and we see that the shapes are independent of the incident energy within the experimental errors. This is what one expects from the impulse approximation (IA). In the IA the QE cross section is

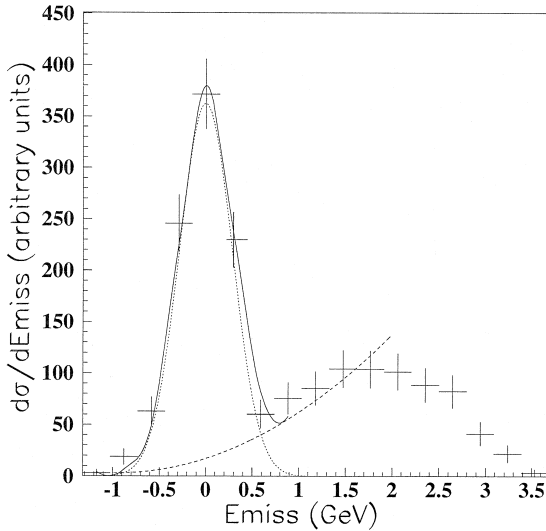


Fig. 1. E_{miss} distribution for 6 GeV/c, $0.1 < |p_{Fy}| < 0.2$ GeV/c, and $|\alpha - 0.87| < 0.05$. The Gaussian (dotted line) represents the QE events. The shape of the background (dashed curve) was deduced from extra track events. The fall-off above 1.5 GeV is an artifact of the trigger. The solid curve is the result of the fit (see text).

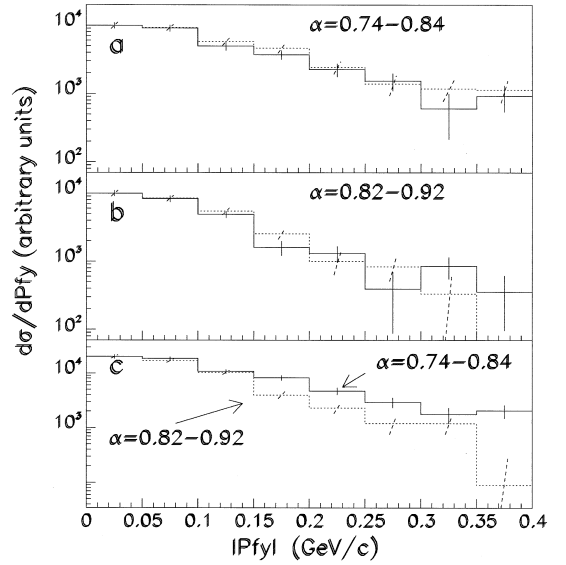


Fig. 2. a-b: $|p_{Fy}|$ distributions for different α slices. The 6 GeV/c (solid line) and the 7.5 GeV/c (dashed line) distributions were normalized at $p_{Fy} = 0$. The slanted error bars are for the 7.5 GeV/c data. c: $|p_{Fy}|$ distributions for $\alpha = 0.79$ (solid line) and for $\alpha = 0.87$ (dashed line). The graphs in each α range are the combined data for 6 and 7.5 GeV/c (see text). The two distributions are normalized at $p_{Fy} = 0$.

factorized into contributions from the probability to find a nucleon with momentum \mathbf{p}_F in the nucleus $n(p_{Fz}, \mathbf{p}_{Ft})$, the free pp elastic cross section and the nuclear transparency $T(s, t)$:

$$\frac{d^3\sigma}{d\mathbf{p}_F}(s, t)_{\text{q.e.}} = \int \frac{d\sigma}{dt}(s, t)_{\text{free}} \cdot n(p_{Fz}, \mathbf{p}_{Ft}) \cdot T(s, t) dt, \quad (1)$$

where t is the Mandelstam variable which represents the squared momentum transfer. For scattering at $\theta_{\text{cm}} \approx 90^\circ$ the free cross section is a function of s only. To obtain a better physical understanding of the kinematics, one may observe that α and s are closely related. Setting $E_F \approx m$, we can write $\alpha \approx 1 - p_{Fz}/m$, and with the additional good approximation in our kinematical region $E_0 = p_0$, we can write:

$$s \sim m^2 + \tilde{m}^2 + 2mp_0\alpha, \quad (2)$$

where E_0 and p_0 are the energy and momentum of

the incident proton and \tilde{m} is the off-mass-shell mass of the target nucleon. Setting $\tilde{m} \simeq m$:

$$s \sim 2m^2 + 2mp_0\alpha. \quad (3)$$

This makes s proportional to α . Within the limited kinematical range of this measurement this approximation is better than 2%. For a given incident momentum, a wide cut on the p_{Fx} component covering the whole distribution and a narrow region of α corresponding to a narrow region of s , we can then write:

$$\frac{d^2\sigma}{dp_{Fy}}(\alpha)_{\text{q.e.}} = n(p_{Fy}) \cdot \text{Factor}(\alpha), \quad (4)$$

where the normalization factor depends on the beam energy. This means, that for fixed α , the $|p_{Fy}|$ distributions at the two incident energies will scale as can be seen clearly in Fig. 2. For small α (Fig. 2 b) the p_{Fz} is about 200 MeV/c and, since the scaling holds also for large p_{Fy} , the scaling has been checked up to fairly large nucleon momenta (about 0.5 GeV/c). The scaling tells us that the $|p_{Fy}|$ distribution remains unchanged even though the cross section on the left of Eq. (4) changes by almost an order of magnitude between 6 and 7.5 GeV/c incident beam.

In Fig. 2c we compare the transverse momentum distributions for two different α ranges. Since the shapes were shown to be independent of the incident energies we combined the measured distributions for the two incident energies. We observe that the transverse momentum distribution gets wider for larger longitudinal momentum in the beam direction (smaller α). ratios of events between This is opposite of what one would expect from a simple Fermi gas model, where the transverse component gets narrower as α approaches values corresponding to the Fermi surface region. It is also incompatible with a Gaussian distribution where transverse and longitudinal components are independent. It is, however, consistent with a distribution with a large momentum tail above the Fermi sea, as expected from two-nucleon short range correlations in nuclei [3,4]. To quantify the statements about the transverse momentum distribution, we present in Table 1 the ratios of events between $200 < |p_{Fy}| < 400$ MeV/c and $0 <$

Table 1

The ratios of events between $200 < |p_{Fy}| < 400$ MeV/c and $0 < |p_{Fy}| < 200$ MeV/c

α range	Incident momentum [GeV/c]	$\frac{200 < p_{Fy} < 400}{0 < p_{Fy} < 200}$ p_{Fy} in [MeV/c]	Shown in Fig.
0.74–0.84	6	0.19 ± 0.03	2a
	7.5	0.21 ± 0.05	2a
	sum	0.20 ± 0.03	2c
0.82–0.90	6	0.12 ± 0.02	2b
	7.5	0.08 ± 0.02	2b
	sum	0.10 ± 0.02	2c

$|p_{Fy}| < 200$ MeV/c for two incident energies and two different α ranges. We also show the ratios for the distribution obtained by summing the measured distributions for the two incident energies. As one can see there is consistency between ratios measured at different energies and the same α range (scaling prediction) and there is a significant difference between the measurements at two different α ranges.

As we mentioned in the introduction, the large momentum transfer QE ($p, 2p$) reaction prefers small s (small α) due to the strong s dependence of the elementary pp elastic cross section. The flux factor for the quasi-elastic pp cross section is different from the free pp one, due to the motion of the target proton in the nucleus. There is also a Jacobian that has to be included when changing reference frames. Taking these effects into account, we obtained the nuclear momentum distribution, $n(p_{Fz})$, by multiplying the measured α distribution, $\Delta N/\Delta\alpha$, by the factor of Eq. (5):

$$n(p_{Fz}) \propto \frac{\Delta N}{\Delta\alpha} \left(\frac{E_2 - p_{2z}}{mp_1} \times \frac{1}{s(s - 4m^2) \left(\frac{d\sigma}{dt} \right)_{p_{1t} = -p_{2t}}} \right) \quad (5)$$

where $\frac{d\sigma}{dt}_{pp}$ is the measured free pp cross section [12], p_1 is the momentum of one of the outgoing

protons, E_2 and p_{2z} are the energy and z momentum component of the other one, p_{1t} and p_{2t} are the transverse components of the two outgoing particles and all the kinematical quantities are in the laboratory frame. A derivation of the factor is given elsewhere [10].

After this correction the α distributions at 6 and 7.5 GeV/c were consistent with each other in shape, as can be seen in the upper part of Fig. 3. We combined the two sets of measurements, as shown in Fig. 3 which, up to distortion from initial and final state interactions and by using the standard non-relativistic description of the nucleus, represents the p_{Fz} distribution of the target nucleon. The value of p_{Fz}

is limited to 280 MeV/c due to a software cut which was applied to ensure a uniform angular acceptance for all target positions. The errors drawn in Fig. 3 contain, in addition to the statistical errors, also the uncertainties in the background subtraction and in the normalization factor of Eq. (5) where measured quantities were used. We see that the errors on the longitudinal distributions at the largest values of p_{Fz} are still small, due the enhancement from the s-dependent weighting.

Just for comparing with the p_{Fz} distribution, we show in Fig. 3 the transverse distribution which was obtained by adding the p_{Fy} distributions, weighted according to the integrated number of events in the relevant α regions. We see that the longitudinal and the transverse distributions have about the same shape even though multiple scattering effects and nuclear transparencies could affect them in different ways.

Also in Fig. 3, to set the scale for the magnitude of the large momentum components, the data are compared to a simple independent particle Fermi motion distribution. A harmonic oscillator model (HO) was used with parameters fitted to ^{12}C electron scattering data with the kinematical constraints of our measurement [13]. As can be seen clearly, the scale of large momentum tails is well above the level indicated by the naive HO model. In order to quantify this statement, we present the ratio between the number of events with $154 < p_{Fz} < 280$ MeV/c and the number of events with $0 < p_{Fz} < 154$ MeV/c (we measured events with $p_{Fz} > 0$ and we assumed that the distribution is symmetric about $p_{Fz} = 0$). The measured ratio is $(29 \pm 2)\%$. The HO prediction for the same ratio is only 11.7%.

In conclusion, the QE events were identified and we showed that it is possible to separate the nuclear properties (ground state momentum distribution) from the reaction mechanism up to a target nucleons total momentum of about 0.5 GeV/c. Based on this result, we deduced the light cone transverse momentum and α distributions up to large momenta. We also show a coupling between the two distributions. The width of the transverse distribution increases for decreasing α (increasing p_{Fz}). The tails of these distributions are consistent with electron scattering data [14]. For comparison, we add to Fig. 3 a curve which represents the experimental $F(y)$ for inclusive electron scattering on ^{12}C as a function of the y

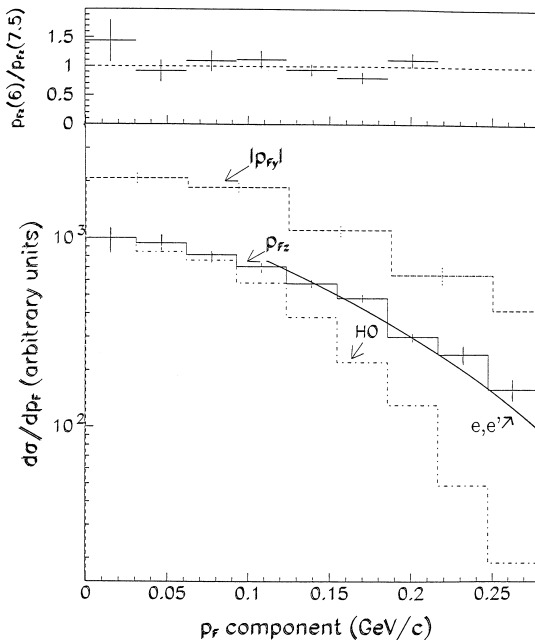


Fig. 3. The upper part of the figure shows the ratio of the two distributions measured at 6 and 7.5 GeV/c (the last two highest momentum points were measured at 6 GeV/c only). p_{Fz} is the longitudinal ground state momentum distribution, obtained from the α distributions for 6 and 7.5 GeV/c combined, after correction for the s dependence induced by the elementary free cross section. The $|p_{Fy}|$ is the transverse distribution extracted from several α regions (see text). HO is a harmonic oscillator independent particle model calculation. The p_{Fz} and HO distributions are normalized to 1000 at the first bin. The curve is the electron scattering $F(y)$ distribution described in the text and is arbitrarily normalized in order to compare its shape to the present data.

scaling variable which, in the limit of large momentum transfer, provides a measure for the longitudinal momentum distribution of the nucleon. Those data are for the momentum transfer range of 1.1 to 1.49 $(\text{GeV}/c)^2$ and for $y = -0.1$ to -0.3 GeV/c . (see Fig. 2 of [14]). Our measured momentum tails are larger than predicted by independent particle models and are characteristic for nucleon-nucleon short range correlations.

Acknowledgements

Very special thanks are due to Dr. M. Sargsyan, who accompanied our analysis with detailed calculations. We wish to thank Drs. L. Frankfurt, M. Strikman, G. Miller for their theoretical input and Drs. D. Day and J. Arrington for supplying us with the inclusive (e,e') data. S. Baker, F.J. Barbosa, S. Kaye, M. Kmit, D. Martel, D. Maxam, J.E. Passaneau, M. Zilca contributed significantly to the design and construction of the detector. We are pleased to acknowledge the assistance of the AGS staff in building the detector and supporting the experiment, particularly our liaison engineers, J. Mills, D. Dayton, C. Pearson. We acknowledge the continuing support of D. Lowenstein and P. Pile. This research was supported by the U.S – Israel Binational Science Foundation, the Israel Science Foundation founded by the Israel Academy of Sciences and Humanities, NSF grant PHY-9501114 and Department of Energy grants DEFG0290ER40553.

References

- [1] A.S. Carroll et al., Phys. Rev. Letters 61 (1988) 1698; S. Heppelmann et al., Phys. Lett. B 232 (1989) 167.
- [2] A. Mueller, in: J. Tran Thanh Van (Eds.), Proc. XVII Rencontres de Moriond (Les Arcs, France, 1982), Editions Frontieres, Gif-sur-Yvette, 1982 p. 13; S.J. Brodsky, in: E.W. Kittel, W. Metzger, A. Stergiou (Eds.), Proc. XIII Intern. Symp. on Multi-particle Dynamics, World Scientific, Singapore, 1982, p. 963. P. Jain, B. Pire, J.P. Ralston, Physics Reports 271 (1996) 67.
- [3] L.L. Frankfurt, M.I. Strikman, Phys. Rep. 160 (1988) 235.
- [4] L.L. Frankfurt et al., Phys. Rev. C 48 (1993) 2451.
- [5] G.R. Farrar et al., Phys. Rev. Letters 62 (1989) 1095.
- [6] S.J. Brodsky, G.R. Farrar, Phys. Rev. Letters 31 (1973) 1153.
- [7] N.C.R. Makins et al., Phys. Rev. Letters 72 (1994) 1986.
- [8] M.A. Shupe et al., EVA, a solenoidal detector for large angle exclusive reactions: Phase I - determining color transparency to 22 GeV/c . Experiment E850 Proposal to Brookhaven National Laboratory, 1988, unpublished.
- [9] Measurement of the dependence of the $C(p,2p)$ cross section on the transverse component of the spectral momentum, S. Durrant, Ph.D. thesis, Pennsylvania State University, 1994, unpublished.
- [10] Quasi-Elastic Hadronic Scattering at Large Momentum Transfer, Y. Mardor, Ph.D. thesis, Tel Aviv University, 1997, unpublished.
- [11] The EVA Trigger: Transverse momentum selection in a solenoid, J.Y. Wu et al., Nuclear Instruments and Methods A 349 (1994) 183–196.
- [12] Compilation of Nucleon - Nucleon and Nucleon - Antinucleon Elastic Scattering Data. M.K. Carter, P.D.B. Collins, M.R. Whalley. Rutherford Lab. publication PAL-86-002, 1986.
- [13] M. Sargsyan, Private Communication; H. Bidasaria, P.M. Fishbane, J.V. Noble, Nucl. Phys. A 355 (1981) 349.
- [14] D. Day et al., Phys. Rev. Lett. 59 (1987) 427.